A singular value homotopy for finding critical parameter values

J.B. Collins [*] Jonathan D. Hauenstein [†]

May 18, 2020

Abstract

Various applications in science and engineering depend upon solving nonlinear systems of equations which depend upon parameters. Locally in the parameter space, the qualitative behavior of the solutions remains the same except at critical parameter values. This article develops a singular value homotopy that aims to compute critical parameters values. Several examples are presented including computing critical parameter values for nonlinear boundary value problems, turning points for a steady-state system connected to learning and memory, and computing the maximum Gaussian curvature of a surface.

1 Introduction

Systems of equations arising in science and engineering typically depend upon parameters such as temperature, pressure, concentration, and length. The solutions to these equations vary with the parameters with the implicit function theorem, e.g., see [22, Thm. A.2.8], showing that the qualitative behavior of the solutions remains the same except at critical parameter values. Therefore, computing critical parameter values is important for creating a complete understanding of the solutions over the parameter space.

Two main applications that benefit from computing critical parameter values are steady-state bifurcations and differential equations with a multiplicity of solutions. Bifurcation diagrams demonstrate the steady-state solutions of differential equations as they depend on one or more parameters of the equations. While most points on a bifurcation diagram can be found through typical computations, the critical parameter values correspond to limit points or turning points which are more difficult to compute as this is where the number of solutions change. Most of the work in determining bifurcation diagrams is in finding these critical parameter values [24].

Many nonlinear differential equations can be shown to have multiple solutions for a particular range of parameter values. For instance, the two-point boundary value problem

$$\begin{aligned} y''(x) &= -\lambda(1+y^2), \qquad 0 < x < 1 \\ y(0) &= 0 \\ y(1) &= 0 \end{aligned} \tag{1}$$

[*]Department of Mathematics, University of Mary Washington (jcollin2@umw.edu)

[†]Department of Applied and Computational Mathematics and Statistics, University of Notre Dame (hauenstein@nd.edu, www.nd.edu/∼jhauenst). This author was partially supported by NSF grant CCF-1812746 and ONR grant N00014-16-1-2722.

is known to have a critical parameter value $\lambda^* > 0$ such that there are two solutions for $0 < \lambda < \lambda^*$ and no solutions for $\lambda > \lambda^*$ [15, 17]. While the existence of such a critical parameter value λ^* is known, there is typically no analytical method for computing the value. Therefore, it is left to numerical methods to approximate λ^* via discretization.

Since the computation of critical parameter values is used in a variety of contexts, there are numerous approaches such as [6, 7, 12, 20]. In this work, we develop a homotopy continuation algorithm (see [5, 22] for a general overview) based on the singular value decomposition which aims to drive the minimum singular value of the Jacobian matrix to zero corresponding to a critical parameter value. This idea can be easily modified when the Jacobian matrix is symmetric, the minimum singular value is degenerate, i.e., has two or more linearly independent singular vectors, or to create a degenerate singular value.

The structure of the paper is as follows. Section 2 provides a short introduction to homotopy continuation and discretization. Section 3 describes the singular value homotopy and some modifications. Section 4 presents several applications of the singular value homotopy applied to differential equations.

2 Homotopy continuation and discretization

The following provides some background information on homotopy continuation and the discretization of differential equations.

2.1 Homotopy continuation and path tracking

The essential idea of homotopy continuation, e.g., see [5, 22] for more details, is to track along a solution path over a segment which, without loss of generality, we may assume is the interval $[0, 1]$. In particular, suppose that $H(y; t) = 0$ is a system of n analytic equations with variables $y = (y_1, \ldots, y_n)$ and parameter $t \in [0, 1]$. Let $J_y H(y; t)$ and $J_t H(y; t)$ be the Jacobian matrix and vector with respect to y and t, respectively. Suppose that one is given a point z such that $H(z; 1) = 0$ and $J_y H(z; 1)$ is invertible, i.e., z is a nonsingular solution of $H(\bullet; 1) = 0$. Then, the implicit function theorem shows that there is an analytic solution path $y(t)$ such that $y(1) = z$ and $H(y(t); t) \equiv 0$ for t in an open neighborhood of 1. In particular, this open neighborhood can be extended from 1 towards 0 until there exists $t^* < 1$ such that either

$$\lim_{t \to (t^*)^+} \|y(t)\| = \infty \quad \text{or} \quad \det J_y H(y(t^*); t^*) = 0. \tag{2}$$

If there is no $t^* \in (0, 1]$ such that (2) occurs, then the path $y(t)$ is said to be trackable [14, Defn. 4.5]. Therefore, one can use predictor-corrector path tracking methods as illustrated in Figure 1 to compute $y(t)$ for $t \in (0, 1]$ as well as the endpoint

$$y(0) = \lim_{t \to 0^+} y(t).$$

Since $H(y(t); t) \equiv 0$, the predictor part arises from applying standard numerical solvers for ordinary differential equations, e.g., Euler or Runge-Kutta, to

$$\frac{d}{dt} H(y(t); t) \equiv 0 \qquad \Longrightarrow \qquad \dot{y}(t) = -J_y H(y(t); t)^{-1} \cdot J_t H(y(t); t). \tag{3}$$

Given a fixed value of t and a numerical approximation of $y(t)$, the corrector part arises from applying standard local numerical solvers, e.g., Newton's method, to $H(\bullet; t) = 0$.

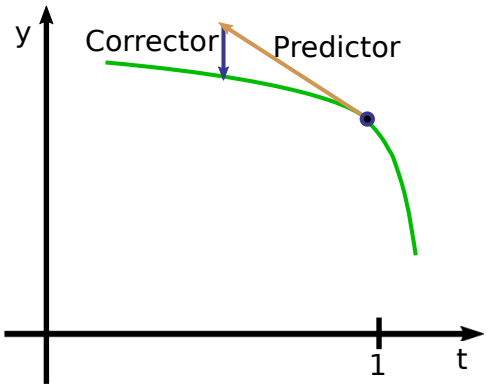

Figure 1: Illustration of predictor-corrector path tracking for path $y(t)$.

Example 1. As an illustrative example, consider $H(y;t) = y^2 - t$ with $z = 1$. Clearly, the analytic solution path $y(t)$ with $y(1) = 1$ and $H(y(t);t) \equiv 0$ is $y(t) = \sqrt{t}$. Since the critical parameter value is $t^* = 0$, this solution path is trackable with

$$\dot{y}(t) = \frac{1}{2y(t)}.$$

For singular endpoints, i.e., $y(0)$ such that $J_y H(y(0);0)$ is singular, endgame procedures (see [22, Chap. 10] for a general overview) can be used to produce accurate approximations of $y(0)$.

2.2 Discretizing differential equations

For parameterized systems of differential equations, critical parameter values are of great interest for fully describing their bifurcation diagrams or finding where the number of solutions changes [10, 17, 18, 21]. One way to construct systems of equations from differential equations which can be used to numerically approximate critical parameter values is by using the finite difference method [2, 9, 16].

The problems presented in Section 4 utilize finite difference discretization to construct systems of equations. To illustrate, consider the boundary value problem (1). Using $n+1$ discretization nodes on the interval $[0,1]$, the spatial step size is $h = (n+1)^{-1}$ and the spatial nodes are $x_j = j \cdot h$ for $j = 0, 1, \ldots, n+1$. Then, y_j denotes an approximation of $y(x_j)$ at each grid point for $j = 1, \ldots, n$ with $y_0 = y_{n+1} = 0$ since $y(0) = y(1) = 0$.

Using a central difference approximation for $y''(x_j)$, namely

$$y''(x_j) \approx \frac{y_{j+1} - 2y_j + y_{j-1}}{h^2},$$

one obtains a system of equations in variables $y = (y_1, \ldots, y_n)$ and parameter λ:

$$\begin{aligned} y_0 - 2y_1 + y_2 + h^2\lambda(1 + y_1^2) &= 0 \\ y_1 - 2y_2 + y_3 + h^2\lambda(1 + y_2^2) &= 0 \\ &\vdots \\ y_{n-1} - 2y_n + y_{n+1} + h^2\lambda(1 + y_n^2) &= 0 \end{aligned} \tag{4}$$

with $y_0 = y_{n+1} = 0$. Therefore, (4) yields a system of n polynomial equations $F(y;\lambda) = 0$ in n variables $y = (y_1, \ldots, y_n)$ and parameter λ.

3 Singular value homotopy

The basic setup is as follows. First, one has a system of n analytic equations $F(y;\lambda) = 0$ in n variables $y = (y_1, \ldots, y_n)$ and parameter λ. Second, one is given a parameter value $\overline{\lambda}$ and a nonsingular solution $\overline{y}$ to $F(\bullet;\overline{\lambda}) = 0$. With this setup, the goal is to track along the solution path through $\overline{y}$ to find a critical parameter value λ^* which is a parameter value such that $F(\bullet;\lambda^*) = 0$ has a singular solution, i.e., a solution with a singular Jacobian matrix $J_y F$.

A common technique used in a variety of problems, e.g., [3, 6, 7, 11, 12, 20], is to incrementally move, i.e., "sweep," along the solution path looking for critical parameter values. This is inherently sensitive to how one numerically steps along the solution path and the numerical criterion for identifying critical parameter values. Therefore, an alternative is to use a homotopy that forces the determinant of the $n \times n$ Jacobian matrix $J_y F$ to be zero. Due to potential numerical computational issues with evaluating and differentiating $\det J_y F$ when n is large, we instead propose a homotopy-based approach based on the minimum singular value. Although this adds more variables and equations, the highly-structured nature of the equations permits large-scale computations as demonstrated on examples in Section 4.

Since the applications in Section 4 depend on tracking real solution paths and computing real solutions, we formulate everything in terms of real computations. The singular value decomposition of a matrix $A \in \mathbb{R}^{n\times n}$ is

$$A = U \cdot \Sigma \cdot V^T$$

where $U, V \in \mathbb{R}^{n\times n}$ are orthogonal, i.e., $U^T \cdot U = V^T \cdot V = I$, and

$$\Sigma = \begin{bmatrix} \sigma_1 & & \\ & \ddots & \\ & & \sigma_n \end{bmatrix} \in \mathbb{R}^{n\times n}$$

such that $\sigma_1 \geq \cdots \geq \sigma_n \geq 0$. The columns of U and V are called the left and right singular vectors, respectively, and the nonnegative numbers $\sigma_1, \ldots, \sigma_n$ are called the singular values. The Eckart-Young theorem [8] shows that σ_n is equal to the 2-norm distance between A and the set of singular $n \times n$ matrices. Moreover, a correlating set of left and right singular vectors and singular value (u_i, v_i, σ_i) satisfies

$$u_i^T \cdot u_i = v_i^T \cdot v_i = 1, \qquad A \cdot v_i = \sigma_i \cdot u_i, \qquad \text{and} \qquad A^T \cdot u_i = \sigma_i \cdot v_i. \tag{5}$$

If $\sigma_i \neq 0$, then $u_i^T \cdot u_i = 1$ is redundant. Removing it from (5) results in $2n+1$ equations in the $2n+1$ variables (u_i, v_i, σ_i). A singular value σ_i is called nondegenerate if there is unique (up to sign) left and right singular vectors u_i and v_i. In Section 3.1, we consider the case when the minimum singular value σ_n is nondegenerate with Section 3.3 considering the degenerate case. Section 3.4 considers the case of making a singular value degenerate. A simplification for the symmetric case, i.e., when $A^T = A$, is provided in Section 3.2.

3.1 Construction of singular value homotopy

With this setup, the following homotopy aims to drive the minimum singular value to zero:

$$H(y,u,v,\lambda;t) = \begin{bmatrix} F(y;\lambda) \\ J_yF(y;\lambda)\cdot v - \sigma(t)\cdot u \\ J_yF(y;\lambda)^T\cdot u - \sigma(t)\cdot v \\ v^T\cdot v - 1 \end{bmatrix} = 0. \tag{6}$$

The start point $(\overline{y},\overline{u},\overline{v},\overline{\lambda})$ at $t=1$ and $\sigma(t)$ are constructed as follows. Since $\overline{y}$ and $\overline{\lambda}$ are given such that $J_yF(\overline{y};\overline{\lambda})$ is full rank, let $\overline{\sigma}_n$ be minimum singular value of $J_yF(\overline{y};\overline{\lambda})$ with corresponding left and right singular vectors $\overline{u}$ and $\overline{v}$, respectively. Finally, $\sigma(t) = t\cdot\overline{\sigma}_n$.

As with iterative methods such as Newton's method, the starting solution $(\overline{y},\overline{\lambda})$ will impact the trackability of the corresponding solution path to (6). In particular, there is no guarantee that the corresponding solution path will be trackable (as defined in Section 2.1) as shown in Ex. 3. However, if the path is trackable and the endpoint is finite, then the solution path ends at a point yielding a critical parameter value. This is summarized in the following.

Theorem 1. With the setup above, if the solution path for H in (6) starting at $(\overline{y},\overline{u},\overline{v},\overline{\lambda})$ is trackable for $t\in(0,1]$ and the endpoint (y^*,u^*,v^*,λ^*) is finite, then λ^* is a critical parameter value such that y^* is a singular solution of $F(\bullet;\lambda^*)=0$.

Proof. Note that trackable solution paths to a homotopy defined by real equations that start at a real point remain real over $t\in(0,1]$. Hence, the result follows since H ensures $F(y^*;\lambda^*)=0$ and 0 is a singular value of $J_yF(y^*;\lambda^*)$. □

The next two examples are an illustrative example followed by a system where the solution path is not trackable.

Example 2. Consider the polynomial system

$$F(y;\lambda) = \begin{bmatrix} y_1^2+y_2^2-1 \\ y_1+y_2-\lambda \end{bmatrix} = 0$$

which describes the intersection of the unit circle and the family of lines with slope $m=-1$. The following illustrates using (6) with two different starting points to compute critical parameter values in which the line is tangent to the circle as shown in Figure 2.

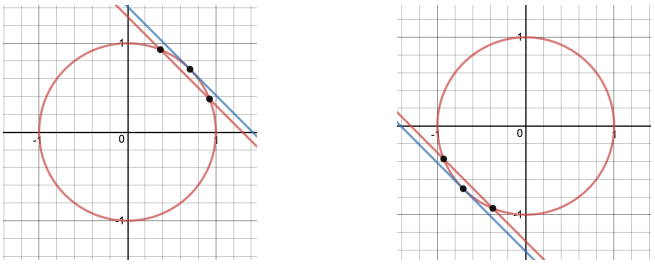

(a) (b)

Figure 2: Computing tangent lines starting with (a) $\overline{\lambda}=1.3$ and (b) $\overline{\lambda}=-1.3$.

First, consider $\overline{\lambda} = 1.3$. Rounding to four decimal places, we take $\overline{y} = (0.9284, 0.3716)$. Then, the minimum singular value of $J_y F(\overline{y}; \overline{\lambda})$ is $\overline{\sigma}_2 = 0.4629$ with left and right singular values $\overline{u} = (0.5661, -0.8243)^T$ and $\overline{v} = (0.4901, -0.8717)^T$, respectively. Applying (6) produces a trackable path which ends with the critical parameter value $\lambda^* = \sqrt{2}$ which corresponds with a line that is tangent to the circle as shown in Figure 2(a).

Similarly, consider $\overline{\lambda} = -1.3$ with $\overline{y} = (-0.9284, -0.3716)$. Then, the minimum singular value of $J_y F(\overline{y}; \overline{\lambda})$ is $\overline{\sigma}_2 = 0.4629$ with left and right singular values $\overline{u} = (0.5661, 0.8243)^T$ and $\overline{v} = (-0.4901, 0.8717)^T$, respectively. Applying (6) produces a trackable path which ends with the critical parameter value $\lambda^* = -\sqrt{2}$ which corresponds with a line that is tangent to the circle as shown in Figure 2(b).

Example 3. Consider the system

$$F(y; \lambda) = \begin{bmatrix} 3y_1 - 1 \\ (1 + \lambda^2) y_2 - 1 \end{bmatrix} = 0 \quad \text{with} \quad J_y F(y; \lambda) = \begin{bmatrix} 3 & 0 \\ 0 & 1 + \lambda^2 \end{bmatrix}.$$

Clearly, for $\lambda \in \mathbb{R}$, $F(y; \lambda) = 0$ has no singular solutions. Thus, every path of a singular value homotopy H in (6) starting at a real solution can not be trackable. For example, with $\overline{\lambda} = 1$ and $\overline{y} = (1/3, 1/2)$, one has $\overline{u} = \overline{v} = (0, 1)^T$ and $\overline{\sigma}_2 = 2$. The corresponding solution path of H in (6) is not trackable at $t = 1/2$. This corresponds with $\lambda = 0$ which is the minimum of $1 + \lambda^2$.

3.2 Symmetric problems

The homotopy H in (6) depends on $3n + 1$ variables. One way to reduce this is to exploit symmetry of the problem. A common structure that arises from discretizations such as the one in (4) is a symmetric Jacobian matrix. When the Jacobian matrix $J_y F(y; \lambda)$ is symmetric, the left and right singular vectors agree up to sign. Hence, one can identify the proper sign choice $\overline{\delta} \in \{+1, -1\}$ based on the start point $(\overline{y}, \overline{\lambda})$ and remove n variables and equations yielding

$$H(y, v, \lambda; t) = \begin{bmatrix} F(y; \lambda) \\ J_y F(y; \lambda) \cdot v - \overline{\delta} \cdot \sigma(t) \cdot v \\ v^T \cdot v - 1 \end{bmatrix} = 0. \tag{7}$$

Theorem 1 can naturally be extended to (7).

3.3 Degenerate minimum singular value

The construction of the singular value homotopy in (6) is applied when the minimum singular value at the start point and along the solution path is nondegenerate. The following considers the degenerate case.

Suppose that $\overline{\sigma}_n$ is the minimum singular value of $J_y F(\overline{y}; \overline{\lambda})$ which we aim to drive to zero. Let $r \geq 1$ be such that $\overline{\sigma}_{n-r+1} = \cdots = \overline{\sigma}_n$, i.e., the minimum singular value $\overline{\sigma}_n$ is repeated r times so that one needs to consider r left and right singular vectors. One obvious generalization of (6) is to replace vectors u and v by $n \times r$ matrices U and V yielding

$$H(y, U, V, \lambda; t) = \begin{bmatrix} F(y; \lambda) \\ J_y F(y; \lambda) \cdot V - \sigma(t) \cdot U \\ J_y F(y; \lambda)^T \cdot U - \sigma(t) \cdot V \\ U^T \cdot U - I \\ V^T \cdot V - I \end{bmatrix} = 0. \tag{8}$$

However, the corresponding starting values of $\overline{U}$ and $\overline{V}$ associated with $\overline{y}$ and $\overline{\lambda}$ need not be isolated as shown in the following.

Example 4. Consider the system

$$F(y;\lambda) = \begin{bmatrix} \lambda(y_1 - 1) \\ \lambda(y_2 - 1) \end{bmatrix} = 0 \quad \text{with} \quad J_y F(y;\lambda) = \begin{bmatrix} \lambda & 0 \\ 0 & \lambda \end{bmatrix}.$$

For $\overline{y} = (1,1)$ and $t = \overline{\lambda} = \overline{\sigma}_1 = \overline{\sigma}_2 = 1$, i.e., $r = 2$, the constraints from (8) on $\overline{U}$ and $\overline{V}$ simplify to $\overline{U} = \overline{V}$ and $\overline{U}^T \cdot \overline{U} = I$ which defines the one-dimensional family of 2×2 orthogonal matrices.

Since path tracking using (3) needs the Jacobian matrix with respect to the variables to be nonsingular, this implies that the solution is isolated. Therefore, one needs to remove the extra degrees of freedom as illustrated in Ex. 4. Theoretically, this is accomplished by working in a corresponding Grassmannian which is a space whose points correspond with linear spaces. To avoid ununnecessary technical details, the following works on an affine patch of the Grassmannian [4]. The key observation is that, for any invertible $r \times r$ matrix K, the following sets of equations are equivalent:

$$\begin{array}{rcl} J_y F(y;\lambda) \cdot V & = & \sigma(t) \cdot U \\ J_y F(y;\lambda)^T \cdot U & = & \sigma(t) \cdot V \end{array} \quad \text{and} \quad \begin{array}{rcl} J_y F(y;\lambda) \cdot V \cdot K & = & \sigma(t) \cdot U \cdot K \\ J_y F(y;\lambda)^T \cdot U \cdot K & = & \sigma(t) \cdot V \cdot K. \end{array}$$

One approach to remove this freedom is to write the $n \times r$ matrix U in a particular way. Since U has rank r, one can always pick K to be the inverse of an $r \times r$ submatrix of U. Therefore, we can select a permutation matrix $P \in \mathbb{R}^{n \times n}$ and write

$$U(\Lambda) = P \cdot \begin{bmatrix} I \\ \Lambda \end{bmatrix} \tag{9}$$

where Λ is an $(n - r) \times r$ matrix of variables. The disadvantage of this representation is that one loses the orthogonality of both $U(\Lambda)$ and corresponding V. Therefore, (8) simplifies to

$$H(y, \Lambda, V, \lambda; t) = \begin{bmatrix} F(y;\lambda) \\ J_y F(y;\lambda) \cdot V - \sigma(t) \cdot U(\Lambda) \\ J_y F(y;\lambda)^T \cdot U(\Lambda) - \sigma(t) \cdot V \end{bmatrix} = 0 \tag{10}$$

where $U(\Lambda)$ as in (9) and $\sigma(t) = t \cdot \overline{\sigma}_n$ as before. Although $U(\Lambda)$ and V are not orthogonal, one still maintains the relationship

$$U(\Lambda)^T \cdot U(\Lambda) = V^T \cdot V. \tag{11}$$

One can easily translate between the two representations: (1) orthogonal U and V typically computed by singular value decomposition algorithms and (2) Λ and V satisfying (11). Suppose that (U_o, V_o) and (Λ_p, V_p) are two such representations, respectively.

Given (U_o, V_o), one can compute a permutation matrix $Q \in \mathbb{R}^{n \times n}$ such that the first r rows of $Q \cdot U_o$ form an invertible $r \times r$ matrix, say K. Let $M \in \mathbb{R}^{(n-r) \times r}$ such that

$$Q \cdot U_o = \begin{bmatrix} K \\ M \end{bmatrix}.$$

Then, $P = Q^T$, $\Lambda_p = M \cdot K^{-1}$ and $V_p = V_o \cdot K^{-1}$ so that $U_o = U(\Lambda_p) \cdot K$ and $V_o = V_p \cdot K$.

Conversely, given (Λ_p, V_p), compute a QR decomposition $V_p = Q \cdot R$ where $Q \in \mathbb{R}^{n\times r}$ orthogonal and $R \in \mathbb{R}^{r\times r}$ upper triangular and invertible. Then, both $U_o = U(\Lambda_d) \cdot R^{-1}$ and $V_o = V_d \cdot R^{-1} = Q$ are orthogonal.

Theorem 1 can naturally be extended to (10). Moreover, note that (10) has $n+2nr$ equations in $n + 2nr + 1 - r^2$ variables. Since this is overdetermined for $r > 1$, [13] provides adaptive techniques for constructing a well-constrained homotopy.

Example 5. Reconsider the system from Ex. 4. Using the orthogonal approach from (8), one has $\overline{U} = \overline{V}$ is any 2×2 orthogonal matrix. However, for (10), one has $n = r = 2$ so that one can take $P = I$ and there is no Λ. Hence, one has $U(\overline{\Lambda}) = I$ and $\overline{V} = I$ at the start point. Running the homotopy (10) yields a trackable path that ends at a critical parameter value $\lambda^* = 0$.

3.4 Two equal singular values

The previous approaches were focused on driving the minimum singular value to zero. However, this method can be easily modified to instead drive two consecutive singular values towards each other using the following homotopy:

$$H(y,u,v,\sigma,\mu,\nu,s,\lambda;t) = \left[\begin{array}{c} F(y;\lambda) \\ \hline J_yF(y;\lambda)\cdot v - \sigma\cdot u \\ J_yF(y;\lambda)^T\cdot u - \sigma\cdot v \\ v^T\cdot v - 1 \\ \hline J_yF(y;\lambda)\cdot \nu - s\cdot\mu \\ J_yF(y;\lambda)^T\cdot \mu - s\cdot\nu \\ \nu^T\cdot\nu - 1 \\ \hline \sigma - s - t\cdot(\overline{\sigma}-\overline{s}) \end{array}\right] = 0. \tag{12}$$

In particular, the second and third blocks of equations enforce that (u, v, σ) and (μ, ν, s) are both correlating collections of left and right singular vectors and singular value for the matrix $J_yF(y;\lambda)$. The last equation aims to drive singular values σ and s together where $\overline{\sigma}$ and $\overline{s}$ are the corresponding starting values.

A natural extension of Theorem 1 can be applied to (12).

4 Numerical results

The following presents four applications of singular value homotopies for differential equations. The first two are boundary value problems. The third is a biological model for signal transduction and gene network used to study long-term memory. The last is a fully nonlinear, second order elliptic partial differential equation which computes a surface of constant Gaussian curvature.

For each of these problems, `Bertini` [5] was used to perform the path tracking. For the boundary value problems, MATLAB was used to determine determine the start point by computing a corresponding singular value decomposition. The start point for the biological model was computed in `Maple`. The Gaussian curvature problem was implemented in `Python`. The start point for the corresponding discretized system was calculated using Newton's method in `Python` which was also used to generate the input files for `Bertini`.

4.1 Boundary value problem

As mentioned in the Introduction, the two-point boundary value problem (1) has a critical parameter value $\lambda^* > 0$ such that (1) has two solutions for $0 < \lambda < \lambda^*$ which merge at λ^* and

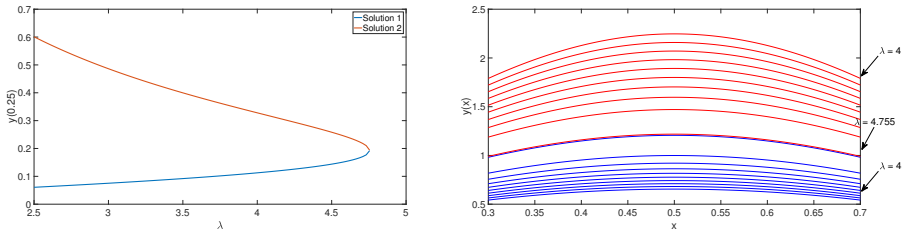

(a) (b)

Figure 3: (a) Plot of $y(0.25)$ for the two solutions to (1) as a function of λ. (b) The two solutions $y(x)$ to (1) plotted for selected values of λ which converge to each other as $\lambda \to \lambda^* \approx 4.755$.

has no solutions for $\lambda > \lambda^*$ as illustrated in Figure 3(a) which plots $y(0.25)$ as a function of λ. For selected values of n, we applied a (symmetric) singular value homotopy to the discretization in (4) to approximate λ^*. To generate a start point, one can, for example, use shooting methods or Newton's method at $\overline{\lambda} = 0.1$ which was chosen to ensure that $\overline{\lambda} < \lambda^*$. Note that [1] suggests $\lambda^* = 4$. Table 1 shows the results of computing λ^* for various values of n showing that the theoretical value of λ^* is approximately 4.755 and Figure 3(b) shows how the two solutions $y(x)$ to (1) converge to each other as $\lambda \to \lambda^* \approx 4.755$.

n	λ^*
10	4.73438
50	4.75415
100	4.75476
200	4.75491
400	4.75495

Table 1: Value of λ^* for (1) using increasingly refined discretizations.

4.2 Another boundary value problem

Consider computing radially symmetric solutions $u(x, y)$ on the annulus

$$\Omega = \{(x, y) \mid 1 < x^2 + y^2 < 2\}$$

satisfying the following boundary value problem:

$$\begin{aligned} \Delta u &= -\lambda \left(1 + u + \frac{u^2}{2} + \frac{u^3}{6}\right) && \text{in } \Omega \\ u(x, y) &= x^2 + y^2 && \text{on } \partial\Omega. \end{aligned} \tag{13}$$

Similar to (1), there exists critical parameter value $\lambda^* > 0$ such that there are two solutions for $0 < \lambda < \lambda^*$ which merge at λ^* and no solutions for $\lambda > \lambda^*$ [17]. Using a discretization with a central difference scheme and a singular value homotopy, Table 2 shows that the theoretical value of λ^* is approximately 2.292.

n	λ^*
10	2.28757
50	2.29225
100	2.29240
200	2.29243

Table 2: Value of λ^* for (13) using increasingly refined discretizations.

4.3 Biological example

The next application is to compute bifurcations for the steady-state behavior of a a biological model connected to learning and memory [19]. This model simulates the levels of various proteins that are responsible for long-term facilitation after exposure to serotonin and is mathematically represented by a system of 15 ordinary differential equations with 40 parameters. In particular, [23] studies steady-state behavior under different model parameter values. They utilized singularity theory which generates bifurcation diagrams as one particular parameter, called the bifurcation parameter λ, is varied. The bifurcation parameter was chosen to be the level of serotonin as this is what is most often varied in experiments. Another branch of solutions were found in [12].

Although the original system depended upon rational functions, one can, at steady-state, clear denominators to produce the following parameterized system of 15 polynomial equations in state variables $y_1, \ldots, y_{15}$, bifurcation parameter λ, and other model parameters $k_1, \ldots, k_{39}$:

$$
\begin{aligned}
3.6\lambda - (y_1 - 0.06)(\lambda + 14) &= 0 \\
k_1 + k_2 y_4 y_1^2 - k_7 y_2 y_3 - k_3 y_2 (y_{15} - k_4) - k_5 y_2 &= 0 \\
k_1 + k_2 y_4 y_1^2 - k_7 y_2 y_3 + k_3 y_2 (y_{15} - k_4) - k_5 y_3 &= 0 \\
k_7 y_2 y_3 - k_2 y_4 y_1^2 - k_3 y_4 (y_{15} - k_4) - k_5 y_4 &= 0 \\
k_9 y_7 (y_{12} + k_{29})(y_5 + k_{13}) - k_{12} y_5 - k_{14} y_5 (y_5 + k_{13}) &= 0 \\
k_{10} (y_{12} + k_{29})(y_5 - y_6)(y_5 + k_{13}) - k_{12} y_6 (y_5 - y_6 + k_{11}) &= 0 \\
-k_{14} y_6 (y_5 + k_{13})(y_5 - y_6 + k_{11}) &= 0 \\
k_{15} - \lambda k_{16} y_7 - k_{18} y_7 (y_7 + k_{17}) &= 0 \\
-\lambda k_{19} y_8 + k_{22} (k_{25} - y_8) &= 0 \\
-k_{20} (k_{25} - y_8) y_9 (k_{26} - y_9 - y_{10} + k_{28}) + k_{23} (k_{26} - y_9 - y_{10})(y_9 + k_{28}) &= 0 \\
k_{20} (k_{25} - y_8)(y_{10} + k_{28}) - k_{23} y_{10} (k_{26} - y_9 - y_{10} + k_{28}) &= 0 \\
-k_{21} y_{10} y_{11} (k_{27} - y_{11} - y_{12} + k_{28}) + k_{24} (k_{27} - y_{11} - y_{12})(y_{11} + k_{28}) &= 0 \\
k_{21} y_{10} (k_{27} - y_{11} - y_{12})(y_{12} + k_{28}) - k_{24} y_{12} (k_{27} - y_{11} - y_{12} + k_{28}) &= 0 \\
k_{30} y_3 (1 - y_{13}) - k_{31} k_{32} y_{13} &= 0 \\
k_{33} (y_{12} + k_{29})(1 - y_{14}) - k_{34} k_{32} y_{14} &= 0 \\
k_{35} y_{13}^2 y_{14}^2 + k_{36} (y_{13}^2 + k_{37}^2)(y_{14}^2 + k_{38}^2) - k_{39} y_{15} (y_{13}^2 + k_{37}^2)(y_{14}^2 + k_{38}^2) &= 0
\end{aligned}
$$

All model parameters except k_{35} are fixed to be the constants given in [23] with k_{35} fixed at different values to obtain qualitatively different diagrams. In particular, for $k_{35} = 0.015$, 0.020, and 0.030, we utilized a singular value homotopy to determine a critical parameter value λ^* corresponding with a turning point of the bifurcation diagram for three values of k_{35} from [23].

While [23] only provides drawings without giving explicit values, the values presented in Table 3 appear to be in correspondence with their drawings.

k_{35}	λ^*
0.015	0.116
0.020	0.105
0.030	0.0859

Table 3: Critical level of serotonin λ^* at the turning points of the bifurcation diagrams for selected values of k_{35} from [23].

4.4 Maximum Gaussian curvature

The final application considers $\mathcal{K}$-surfaces which are surfaces with constant Gaussian curvature $\mathcal{K} > 0$. For a domain $\Omega \subset \mathbb{R}^2$ and a function $u(x, y)$, consider the surface $S \subset \mathbb{R}^3$ given by the graph of u over Ω, namely

$$S = \{(x, y, u(x, y)) \mid (x, y) \in \Omega\}. \tag{14}$$

The Gaussian curvature on S is given by

$$\mathcal{K} = \frac{\det(D^2 u)}{(1 + \|\nabla u\|^2)^2}$$

where $D^2 u = u_{xx} u_{yy} - u_{xy}^2$ and $\|\nabla u\|^2 = \nabla u \cdot \nabla u$. Therefore, the surfaces S represented in (14) which have a constant Gaussian curvature $\mathcal{K} > 0$ arise from functions $u(x, y)$ on Ω which solve the following partial differential equation:

$$\begin{aligned} \det(D^2 u) &= \mathcal{K} \cdot (1 + \|\nabla u\|^2)^2 && \text{in } \Omega \\ u(x, y) &= g(x, y) && \text{on } \partial\Omega \end{aligned} \tag{15}$$

for some boundary function $g(x, y)$. Hence, given a domain Ω, boundary function $g(x, y)$, and curvature $\mathcal{K} > 0$, one obtains a $\mathcal{K}$-surface by solving (15). Figures 4 and 5 show solutions to

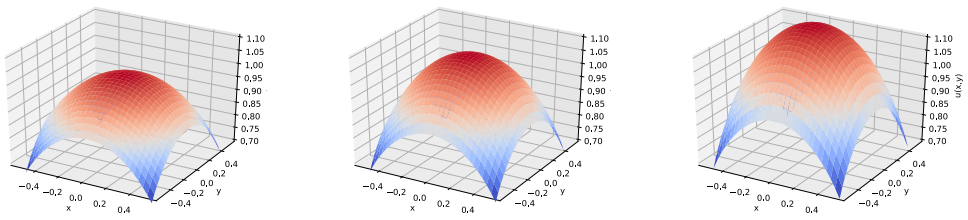

(a) (b) (c)

Figure 4: $\mathcal{K}$-surfaces obtained by solving (15) on $\Omega = [-0.57, 0.57]^2$ with boundary condition $g_1(x, y) = \sqrt{1 - x^2 - y^2}$ and curvature (a) $\mathcal{K} = 1$, (b) $\mathcal{K} = 1.5$, and (c) $\mathcal{K} = 2$.

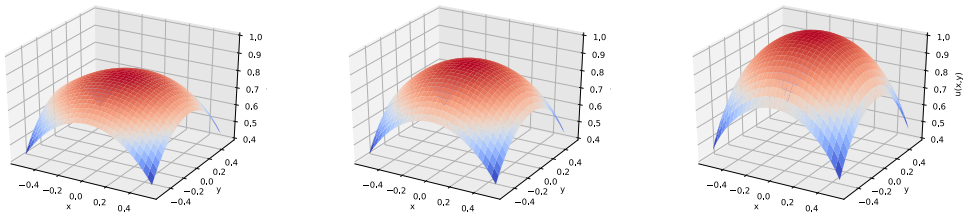

(a) (b) (c)

Figure 5: $\mathcal{K}$-surfaces obtained by solving (15) on $\Omega = [-0.57, 0.57]^2$ with boundary condition $g_2(x, y) = 1 - x^2 - y^2$ and curvature (a) $\mathcal{K} = 1$, (b) $\mathcal{K} = 1.5$, and (c) $\mathcal{K} = 2.2$.

this problem for $\Omega = [-0.57, 0.57]^2$ on two different sets of boundary conditions for various values of $\mathcal{K}$. Moreover, if (15) has a solution for some $\mathcal{K}_0 > 0$, then it has a solution for all $\mathcal{K} \in (0, \mathcal{K}_0]$ [3]. Due to geometric constraints, there is a maximum curvature $\mathcal{K}_{\max} > 0$ for which a well-defined solution to (15) exists for $\mathcal{K} \in (0, \mathcal{K}_{\max}]$ and no solution for $\mathcal{K} > \mathcal{K}_{\max}$. The value of $\mathcal{K}_{\max}$ can be computed explicitly for simple cases, but there is no analytic method for computing $\mathcal{K}_{\max}$ in general. In [3], a type of "sweeping" method was used to approximate $\mathcal{K}_{\max}$ by incrementing the value of $\mathcal{K}$ on a discretization of (15) until some termination criteria suggesting that no solution could exist. However, it is unclear what termination criteria was used.

Since the value of $\mathcal{K}_{\max}$ is a critical parameter value, we utilize a singular value homotopy applied to a discretization to approximate it. Assuming that the domain is rectangular, say

$$\Omega = [a_x, b_x] \times [a_y, b_y],$$

we following a setup similar to Section 2.2. In particular, using $n + 1$ of grid points in each direction, the mesh size in the x and y directions, respectively, are

$$h_x = \frac{b_x - a_x}{n+1} \quad \text{and} \quad h_y = \frac{b_y - a_y}{n+1}.$$

With grid points $x_j = a_x + j \cdot h_x$ and $y_j = a_y + j \cdot h_y$ for $j = 0, \ldots, n+1$, let $u_{i,j}$ be an approximation of $u(x_i, y_j)$. We utilized the following standard discretized approximations:

$$\begin{aligned}
u_{xx}(x_i, y_j) &\approx \frac{u_{i+1,j} - 2u_{i,j} + u_{i-1,j}}{h_x^2}, \\
u_{yy}(x_i, y_j) &\approx \frac{u_{i,j+1} - 2u_{i,j} + u_{i,j-1}}{h_y^2}, \\
u_{xy}(x_i, y_j) &\approx \frac{u_{i+1,j+1} - u_{i-1,j+1} - u_{i+1,j-1} + u_{i-1,j-1}}{4h_x h_y}, \\
u_x(x_i, y_j) &\approx \frac{u_{i+1,j} - u_{i-1,j}}{2h_x}, \\
u_y(x_i, y_j) &\approx \frac{u_{i,j+1} - u_{i,j-1}}{2h_y}.
\end{aligned}$$

To compare with results in [3], we consider two problems from [3] on the square domain $\Omega = [-.57, .57]^2$ with boundary conditions

$$g_1(x, y) = \sqrt{1 - x^2 - y^2} \quad \text{and} \quad g_2(x, y) = 1 - x^2 - y^2. \tag{16}$$

For each boundary condition, we started with the parameter value $\overline{\mathcal{K}} = 1.8$ and computed a starting solution obtained using Newton's method applied to the discretized system. Table 4 shows the computed values for $\mathcal{K}_{\max}$ for selected values of n which are similar to the values reported in [3], namely 2.10 and 2.24, respectively.

$g_1(x, y)$

n	$\mathcal{K}_{\max}$
16	2.12
24	2.085
32	2.07

$g_2(x, y)$

n	$\mathcal{K}_{\max}$
16	2.24
24	2.21
32	2.20

Table 4: Computed values of maximum Gaussian curvature for domain $\Omega = [-.57, .57]^2$ with boundary condition $g_1(x, y)$ and $g_2(x, y)$ from (16) for selected values of n.

5 Conclusion

The singular value homotopy is an approach for determining critical parameter values by forcing the minimum singular value to zero. These critical parameter values are of great interest in many applications as they can determine where the qualitative behavior, such as the number of solutions, can change.

Classical approaches for computing critical parameter values use a "sweeping" approach along the parameter space. For instance, the maximum Gaussian curvature $\mathcal{K}_{\max}$ can be found by find a starting solution for some $\mathcal{K} < \mathcal{K}_{\max}$ and then slowly increasing the parameter value $\mathcal{K}$. The disadvantage of this approach is one has to decide how to increase the parameter and when one reaches the critical parameter value. In [3], $\mathcal{K}$ was increased by a fixed value of $\Delta\mathcal{K} = 0.02$. Using a singular value homotopy, one can utilize homotopy continuation path tracking techniques (e.g., see [5, Chaps. 2-3]) to adaptively determine the step size for predictor-corrector path tracking and endgames to accurately compute the endpoint corresponding with the critical parameter value. A variety of problems arising from differential equations are used to demonstrate some of the many applications of singular value homotopies.

References

[1] E. L. Allgower, D. J. Bates, A. J. Sommese, and C. W. Wampler. Solution of polynomial systems derived from differential equations. *Computing*, 76(1-2):1–10, 2006.

[2] U. M. Ascher and L. R. Petzold. *Computer methods for ordinary differential equations and differential-algebraic equations*, volume 61. Siam, 1998.

[3] F. E. Baginski and N. Whitaker. Numerical solutions of boundary value problems for $\mathcal{K}$-surfaces in $\mathbb{R}^3$. *Numerical Methods for Partial Differential Equations: An International Journal*, 12(4):525–546, 1996.

[4] D. J. Bates, J. D. Hauenstein, C. Peterson, and A. J. Sommese. Numerical decomposition of the rank-deficiency set of a matrix of multivariate polynomials. In L. Robbiano and J. Abbott, editors, *Approximate Commutative Algebra*, pages 55–77. Springer Vienna, Vienna, 2010.

[5] D. J. Bates, J. D. Hauenstein, A. J. Sommese, and C. W. Wampler. *Numerically solving polynomial systems with Bertini*, volume 25 of *Software, Environments, and Tools*. Society for Industrial and Applied Mathematics (SIAM), Philadelphia, PA, 2013.

[6] A. Dhooge, W. Govaerts, and Y. A. Kuznetsov. Matcont: A matlab package for numerical bifurcation analysis of odes. *SIGSAM Bull.*, 38(1):21–22, 2004.

[7] E. Doedel. AUTO: a program for the automatic bifurcation analysis of autonomous systems. *Congr. Numer.*, 30:265–284, 1981.

[8] C. Eckart and G. Young. The approximation of one matrix by another of lower rank. *Psychometrika*, 1:211–218, 1936.

[9] W. Gautschi. *Numerical analysis*. Springer Science & Business Media, 1997.

[10] J. R. Graef, L. Kong, and H. Wang. Existence, multiplicity, and dependence on a parameter for a periodic boundary value problem. *J. Differential Equations*, 245(5):1185–1197, 2008.

[11] W. Hao, J. D. Hauenstein, B. Hu, and A. J. Sommese. A three-dimensional steady-state tumor system. *Applied Mathematics and Computation*, 218(6):2661–2669, 2011.

[12] H. A. Harrington, D. Mehta, H. M. Byrne, and J. D. Hauenstein. Decomposing the parameter space of biological networks via a numerical discriminant approach. In J. Gerhard and I. Kotsireas, editors, *Maple in Mathematics Education and Research*, pages 114–131, Cham, 2020. Springer International Publishing.

[13] J. D. Hauenstein and M. H. Regan. Adaptive strategies for solving parameterized systems using homotopy continuation. *Applied Mathematics and Computation*, 332:19–34, 2018.

[14] J. D. Hauenstein, A. J. Sommese, and C. W. Wampler. Regeneration homotopies for solving systems of polynomials. *Math. Comp.*, 80(273):345–377, 2011.

[15] T. Laetsch. On the number of solutions of boundary value problems with convex nonlinearities. *J. Math. Anal. Appl.*, 35:389–404, 1971.

[16] R. J. LeVeque. *Finite difference methods for ordinary and partial differential equations: steady-state and time-dependent problems*, volume 98. Siam, 2007.

[17] S. S. Lin. Positive radial solutions and nonradial bifurcation for semilinear elliptic equations in annular domains. *J. Differential Equations*, 86(2):367–391, 1990.

[18] N. S. Papageorgiou and G. Smyrlis. A bifurcation-type theorem for singular nonlinear elliptic equations. *Methods Appl. Anal.*, 22(2):147–170, 2015.

[19] D. B. Pettigrew, P. Smolen, D. A. Baxter, and J. H. Byrne. Dynamic properties of regulatory motifs associated with induction of three temporal domains of memory in aplysia. *Journal of computational neuroscience*, 18(2):163–181, 2005.

[20] K. Piret and J. Verschelde. Sweeping algebraic curves for singular solutions. *J. Comput. Appl. Math.*, 234(4):1228–1237, 2010.

[21] J. Shi and M. Yao. On a singular nonlinear semilinear elliptic problem. *Proc. Roy. Soc. Edinburgh Sect. A*, 128(6):1389–1401, 1998.

[22] A. J. Sommese and C. W. Wampler, II. *The numerical solution of systems of polynomials arising in engineering and science*. World Scientific Publishing Co. Pte. Ltd., Hackensack, NJ, 2005.

[23] H. Song, P. Smolen, E. Av-Ron, D. A. Baxter, and J. H. Byrne. Bifurcation and singularity analysis of a molecular network for the induction of long-term memory. *Biophysical journal*, 90(7):2309–2325, 2006.

[24] S. H. Strogatz. *Nonlinear dynamics and chaos*. Westview Press, Boulder, CO, second edition, 2015. With applications to physics, biology, chemistry, and engineering.